AAEC/E465

AAEC/E465

AUSTRALIAN ATOMIC ENERGY COMMISSION

RESEARCH ESTABLISHMENT

LUCAS HEIGHTS

APPROXIMATE FIRST COLLISION PROBABILITIES FOR NEUTRONS IN CYLINDRICAL AND CLUSTER LATTICES

by

G.S. ROBINSON

May 1979

ISBN 0 642 59669 7

AUSTRALIAN ATOMIC ENERGY COMMISSION
RESEARCH ESTABLISHMENT
LUCAS HEIGHTS

APPROXIMATE FIRST COLLISION PROBABILITIES FOR NEUTRONS IN CYLINDRICAL AND CLUSTER LATTICES

by

G.S. ROBINSON

ABSTRACT

Methods for calculating approximate first collision probabilities for neutrons in cylindrical and cluster lattices are presented and compared with numerical solution methods. The methods differ from those of other authors in the inclusion of anisotropic boundary conditions for both geometries. The methods, which are fast enough for routine use in multigroup and resonance subgroup calculations, have been coded in FORTRAN and included in modules of the AUS scheme for reactor neutronics calculations.

National Library of Australia card number and ISBN 0 642 59669 7

The following descriptors have been selected from the INIS Thesaurus to describe the subject content of this report for information retrieval purposes. For further details please refer to IAEA-INIS-12 (INIS: Manual for Indexing) and IAEA-INIS-13 (INIS: Thesaurus) published in Vienna by the International Atomic Energy Agency.

REACTOR LATTICES; REACTORS; CYLINDRICAL CONFIGURATION; FUEL ELEMENT CLUSTERS; NEUTRONS; ANALYTICAL SOLUTION; PROBABILITY; BOUNDARY CONDITIONS; ANISOTROPY; FISSION; A CODES; M CODES; NEUTRON TRANSPORT THEORY

CONTENTS

(Continued)

CONTENTS (Continued)

1. INTRODUCTION

The use of approximate first flight collision probabilities for the calculation of both cylindrical and cluster lattices of a nuclear reactor has been widespread for a number of years. Methods for cylindrical geometry have been developed by Bonalumi [1961, 1965] and Jonsson [1963], and treatments for cluster geometry have been given by Bonalumi [1965], Doherty [1970], BOllacasa & Bonalumi [1970] and Yamamoto & Ishida [1971].

The original work of Bonalumi [1961] on cylindrical geometry was improved in some important aspects by Jonsson [1963]. The next development was a simplification of the approximations without loss of accuracy, and the extension to a non-circular outer boundary [Bonalumi 1965]. The present report describes a method that is based largely on this latter work; it also summarises the approximations of Bonalumi [1965] which have been adopted and details their application to multiregion calculations with anisotropic boundary conditions.

The published treatments of cluster geometry are similar in approach; cluster collision probabilities have been synthesised from pincell calculations for typical fuel rods and a cylindrical calculation using smeared cross sections for the annuli which contain rods. Isotropic boundary conditions have been applied to the pincells to form the composite cluster collision probabilities. The methods differ in the prescription used for the smeared cross sections and in the partition of collision probabilities within the pincells. The main feature of the present method is that anisotropic boundary conditions have been applied to pincells which have been assumed to have polygonal boundaries.

2. CYLINDRICAL GEOMETRY

2.1 General

The system considered is a lattice cell which consists of N concentric annuli numbered from the centre outwards with radii r_i, outer surfaces S_i, volumes V_i and cross sections Σ_i. The outermost radius r_N is that radius which gives the correct cell volume for a regular polygonal cell boundary of n sides. The probability that a neutron born uniformly in region i will have its first collision in region j is denoted P_{ij}. The basic approach to the calculation is:

(a) first to calculate the probabilities for a free boundary and apply appropriate boundary conditions later,

(b) to calculate P_{ij} directly for $j \geqslant i$ and obtain the remainder by reciprocity, and

(c) to calculate P_{ij} for $j > i$ as the product of the escape probability from region i and the striking probability in region j for a neutron isotropically crossing surface i.

2.2 Striking Probability G_{ij}

The first collision probability in region j for neutrons penetrating isotropically through the surface i is denoted by G_{ij}. The calculation of G_{ij} follows that of Bonalumi [1965] to whom reference should be made for the derivation of the formulae quoted. Bonalumi approximates G_{ij} by a pseudo-linear (P-L) approximation in which an integral of the form

$$I = \int_0^{\pi/2} f(t)\,Ki_3(Z)\,dt \quad , \tag{1}$$

where $Z = Z(t)$ and Ki_3 is the Bickley function, is approximated by

$$I = F\,Ki_3(\bar{Z}) \quad , \tag{2}$$

where $$F = \int_0^{\pi/2} f(t)\,dt \quad , \tag{3}$$

and $$\bar{Z} = \frac{1}{F}\int_0^{\pi/2} f(t)Z(t)\,dt \quad . \tag{4}$$

The value of G_{12} for a circular surface S_2 thus obtained is

$$G_{12} = 1 - \frac{4}{\pi}\,Ki_3(\eta_2 S) \quad , \tag{5}$$

where $\eta_2 = \Sigma_2 r_2$,

$$S(\alpha) = \frac{\pi}{4}\left[\frac{2}{\pi}\left(\frac{\arcsin\alpha}{\alpha} + \sqrt{1-\alpha^2}\right) - \alpha\right] \quad , \tag{6}$$

and $\alpha = r_1/r_2$.

The corresponding formula for G_{12}, where S_2 is a polygon of n sides, is

$$G_{12} = 1 - \frac{4}{\pi}\,Ki_3(\eta_2 P) \quad , \tag{7}$$

where $\eta_2 = \Sigma_2 D$.

D is the radius of the circle inscribed in the polygon S_2,

$$P(\alpha,u) = \frac{1}{2\alpha u}\left\{ \arcsin(\alpha \cos u)\tan u + \alpha \log\frac{\alpha+t}{\alpha-t} - \right.$$

$$\left. - \frac{1+\alpha^2}{2} \log\frac{1+t}{1-t} - \frac{\pi}{2}\alpha^2 u \right\} \quad , \qquad (8)$$

$$\alpha = r_1/D \quad ,$$

$$u = \pi/n \quad ,$$

and $$t = \frac{\alpha \sin u}{\sqrt{1-\alpha^2\cos^2 u}} \quad .$$

The generalisation of the above results to the case G_{ij} for $j > i$ is given by

$$G_{ij} = \frac{4}{\pi}\left(Ki_3(x_{i,j-1}) - Ki_3(x_{i,j})\right) \quad , \qquad (9)$$

where $$x_{i,i} = 0 \quad ,$$

$$x_{i,j} = x_{i,j-1} + \Sigma_j\left(r_j S(r_i/r_j) - r_{j-1} S(r_i/r_{j-1})\right) \quad , \quad j \neq N \quad ,$$

$$x_{i,N} = x_{i,N-1} + \Sigma_N\left(D\, P(r_i/D,u) - r_{N-1} S(r_i/r_{N-1})\right) \quad , \qquad (10)$$

and D is half the pitch, given by $D = r_N \Big/ \sqrt{\tan u/u}$.

2.3 Probabilities P_{1j}

The probabilities P_{1j} for neutrons born in the central region are treated as a special case. The self-collision term is given by

$$P_{11} = P_c(\Sigma_1 r_1) \quad , \qquad (11)$$

where P_c is the function tabulated by Case *et al.* [1953] for which accurate subroutines are available. To obtain the remaining probabilities, the approximation made is

$$P_{1j} = (1-P_{11})G_{1j} \quad , \quad j \neq 1 \quad . \qquad (12)$$

That is, the neutrons emitted from the central rod are assumed to penetrate isotropically through the surface S_1. Some data on the accuracy of this assumption are given in the following subsection.

2.4 Self-collision Probabilities P_{ii} for $i > 1$

The self-collision probability for a solid non-circular cylinder of volume V, surface S and cross section Σ is first considered. The method of calculation again follows that of Bonalumi [1965]. The black

and white radii of the cylinder are given, respectively, by

$$r_B = 2V/S \quad \text{and} \quad r_W = \sqrt{V/\pi} \ .$$

The self-collision probability is $P_c(\Sigma r_{eff})$, where r_{eff} is an equivalent radius of the cylinder given by

$$r_{eff} = r_B \left(1 + \frac{a}{1+b\Sigma r_B}\right) \ , \qquad (13)$$

where $a = r_W/r_B - 1$,

and $b = \frac{1}{2}(a+1)$.

These formulae have been retained for polygonal shapes for which more precise values of r_W are known, because the results for the self-collision probability are slightly superior when this r_W value is used with the equivalence principle inherent in Equation (13).

To obtain the self-collision probability P_{ii} for $i > 1$, the approximation used is that of Bonalumi [1961]:

$$P_{ii} = P_{ii}^{(0)} - \underset{j<i}{\text{Sum}} \, P_{ij} G_{i-1,i} \ , \qquad (14)$$

where $P_{ii}^{(0)}$ refers to the case with $\Sigma_j = 0$ for $j < i$. To make use of this expression, the P_{ij} values are calculated in the following order: P_{ij} for $j \geq i$, with P_{ji} for $j > i$ by reciprocity, are calculated for each value of i in turn from 1 to N. It remains to obtain a value for $P_{ii}^{(0)}$.

An accurate prescription for $P_{ii}^{(0)}$ has been given by Schaefer (unpublished, but quoted by Jonsson [1963]) for strictly circular annuli. A method of obtaining $P_{ii}^{(0)}$, which is also valid for a polygonal outer boundary, has been proposed by Bonalumi [1965]. This method considers neutron conservation for a system in which $\Sigma_j = \Sigma_i$ for $j < i$, which is treated as two regions to which Equations (12) and (14) are applied to obtain

$$P_{ii}^{(0)} = \frac{\tilde{P} - \alpha_i^2 [\tilde{P}_1 + G_{i-1,i}(1-\tilde{P}_1)(2-G_{i-1,i})]}{1-\alpha_i^2} \ , \qquad (15)$$

where $\alpha_i = r_{i-1}/r_i$,

$\tilde{P}$ is the self-collision probability for the region $r < r_i$,

and $\tilde{P}_1 = \tilde{P}_c(\Sigma_i r_{i-1})$ is the self-collision probability for the region $r < r_{i-1}$.

Although $P = P_c(\Sigma_i r_i)$ for a circular boundary S_i, the application of Equation (13) to the polygonal boundary of region N yields

$$\tilde{P} = P_c(\Sigma_N r_{eff}) \quad , \tag{16}$$

where $r_{eff} = D+(r_N-D)/(1+\Sigma_N r_N/2)$.

A comparison of the results obtained from Equation (15) for circular annuli with the Schaefer prescription and the exact values obtained using the numerical integration routine of Doherty [1969] is given in Table 1. It can be seen that although the Schaefer values are generally accurate to 1 per cent, there are large errors in the values obtained from Equation (15) for thin annuli. The cause of these errors is the use of the approximation $P_{12} = (1-P_{11})G_{12}$ in deriving Equation (15). This may be seen from Table 2, in which the exact value of G_{12} and the P-L approximation to G_{12} are compared with numerical integration results for $P_{12}/(1-P_{11})$. The P-L approximation to G_{12} is shown to have only a minor deterioration for large $\Sigma_2 r_2$ and r_1/r_2. The error in the approximation $P_{12} = (1-P_{11})G_{12}$, which becomes exact as $P_{11} \to 1$, is quite considerable for some values of the parameters. This error, which is acceptable in P_{12}, becomes magnified in obtaining $P_{ii}^{(0)}$ and is not reduced to any extent in the ultimate values for P_{ii}.

In view of these accuracy considerations, the following procedure has been adopted. For strictly circular annuli, the Schaefer prescription has been used. For an outer polygonal boundary, the Schaefer value obtained with the 'volume equivalent' r_N has been modified by the ratio of the value obtained from Equation (15) for the polygonal outer boundary to that obtained using volume equivalence.

2.5 Probabilities P_{ij} for $i > 1$, $j > i$

To calculate the probabilities for $i > 1$ and $j > i$, the Jonsson [1963] modification to Bonalumi's original formulation [1961] has been followed. In this method, the probability P_{ij} is split into two parts. Those neutrons crossing regions interior to i before colliding in region j, are assumed to penetrate the surface S_{i-1} isotropically. Those neutrons travelling directly outward have an angular distribution resulting in striking probabilities H_{ij}, which are calculated in terms of the G_{ij} by a consideration of a uniform rod of radius r_i and cross

section Σ_i. Reference should be made to Jonsson [1963] for the derivation. The final result is

$$P_{ij} = (1-P_{ii}^{(0)})G_{ij} - \sum_{k<i} P_{ik}G_{i-1,j} + \frac{\alpha_i^2(1-q_i)}{1-\alpha_i^2}(1-G_{i-1,i})\{(1-G_{i-1,i})G_{ij}-G_{i-1,j}\}, \quad (17)$$

where $q_i = P_c(\Sigma_i r_{i-1})$. This expression, which is also quoted by Bollacasa & Bonalumi [1970], is an algebraic simplification of the result of Jonsson.

2.6 Boundary Conditions for a Two-region System

In a multiregion calculation, the probability P_{iB} that a neutron born in region i crosses the cell boundary B is given by

$$P_{iB} = 1-\sum_{j=1}^{N} P_{ij} . \quad (18)$$

In the case in which the neutrons have isotropic angular distribution on the cell boundary, the surface-volume reciprocity relation may be applied to give

$$P_{Bi} = 4V_i\Sigma_i P_{iB}/S_N . \quad (19)$$

The boundary to boundary probability P_{BB} is then given by

$$P_{BB} = 1-\sum_{i=1}^{N} P_{Bi} , \quad (20)$$

and the total lattice collision probabilities P'_{ij} are given by

$$P'_{ij} = P_{ij} + \frac{P_{iB}P_{Bj}}{1-P_{BB}} . \quad (21)$$

To proceed to non-isotropic boundary conditions, the treatment of the Dancoff factor in a two-region system given by Bonalumi [1965] is followed.

The Dancoff correction for a two-region lattice is given by

$$G_u = 1-G_m , \quad (22)$$

where G_m and G_u are the total striking probabilities in the moderator and the fuel rods (which are assumed to be black) for isotropic emission from a fuel rod (region 1). The situation for black rods and isotropic boundary conditions is examined first. It follows immediately that

$$G_u = (1-G_{12})G_{S1}/(G_{S1}+G_{S2}) \quad , \tag{23}$$

where the symbol G_{Si} represents P_{Bi} in the black rod case. To obtain expressions for G_{S1} and G_{S2}, it is noted firstly that

$$\lim_{\Sigma_1 \to \infty} 4V_1\Sigma_1(1-P_{11})/S_1 = 1 \quad . \tag{24}$$

Application of the expressions previously derived for P_{ij} and Equations (18) and (19) then yields

$$\frac{G_{S2}}{G_{S1}} = \theta = y\,\frac{1-P_{22}^{(0)}}{1-G_{12}} - G_{12} \quad , \tag{25}$$

where $y = 4V_2\Sigma_2/S_1$. Thus from Equations (22) and (23), G_m is given by

$$G_m = 1 - \frac{1-G_{12}}{1+\theta} \quad . \tag{26}$$

To include non-isotropic incidence of neutrons on the boundary, it is assumed that

$$\frac{G'_{S2}}{G'_{S1}} = \beta\theta \quad , \tag{27}$$

where the symbol G'_{Si} represents the striking probabilities for non-isotropic incidence on the boundary after birth in region 1, θ is given by Equation (25) and β is supposed to be a function of $\Sigma_2 r_1$ only (for black rods). The value of β is determined from the situation in which the rods are in contact so that $G'_{S1} + G'_{S2} = 1$ and, therefore,

$$G'_{S1} = 1/(1+\beta\theta) \quad . \tag{28}$$

With the rods in contact, the moderator is divided into separate non-circular cylinders to which Equation (13) may be applied to obtain the self-collision probability P_{mm}. Applying surface-volume reciprocity to these moderator cylinders gives

$$\bar{G}_m = \frac{4V_m\Sigma_2}{S_m}(1-P_{mm}) \quad , \tag{29}$$

where the subscript m refers to the moderator cylinders and the bar denotes the rods in contact situation. From Equation (23), which holds for G'_{Si} also,

$$1-\bar{G}_m = \bar{G}_u = (1-\bar{G}_{12})\bar{G}'_{S1} \quad , \tag{30}$$

so that

$$\bar{G}'_{S1} = \frac{1-\bar{G}_m}{1-\bar{G}_{12}} \quad . \tag{31}$$

Thus β is determined from Equation (28) to be

$$\beta = \frac{\bar{G}_{S1}}{\bar{G}_{S2}} \frac{\bar{G}_m-\bar{G}_{12}}{1-\bar{G}_m} \quad , \tag{32}$$

and the Dancoff correction is given by

$$G_m = 1-G_u = 1 - \frac{1-G_{12}}{1+\beta\theta} \quad . \tag{33}$$

The values obtained here for G_m are slightly different from those of Bonalumi because different values have been used for $P_{ii}^{(0)}$. The values for G_m given in Table 3 correspond to those in Table 6 of Bonalumi [1965]. It can be seen that the present values are a slight improvement.

To apply non-isotropic boundary conditions for any value of Σ_1, it is assumed that neutrons crossing S_1 have a probability of colliding in V_1 which is the same for non-isotropic incidence on S_2 as it is for isotropic incidence on S_2. Values of P_{Bi} for any Σ_1 may be related then to G_{Si} for $\Sigma_1 = \infty$ by the equations

$$P_{B2} = G_{S2}+G_{S1}(1-G_{11})G_{12} \quad , \tag{34}$$

$$P'_{B2} = G'_{S2}+G'_{S1}(1-G_{11})G_{12} \quad , \tag{35}$$

$$P_{B1}/G_{S1} = P'_{B1}/G'_{S1} = G_{11} \quad , \tag{36}$$

where

$$G_{11} = \frac{4V_1\Sigma_1}{S_1}(1-P_{11}) \quad , \tag{37}$$

and G'_{Si} and P'_{Bi} represent the non-isotropic situation. The final result from these equations is

$$\frac{P'_{B2}}{P'_{B1}} = \frac{P_{B2}}{P_{B1}} + \frac{(\beta-1)\theta}{G_{11}} \quad , \tag{38}$$

which may be rewritten as

$$\frac{P'_{B2}}{P'_{B1}} = \beta^* \frac{P_{B2}}{P_{B1}} \quad , \tag{39}$$

where

$$\beta^* = \left(1 + \frac{(\beta-1)\theta}{G_{11}}\right) \frac{P_{B1}}{P_{B2}} \quad . \tag{40}$$

As β is a function of a single variable, the above equations have been applied by tabulating β as a function of $\Sigma_2 r_1$. The values of β for square and hexagonal lattices are given in Figure 1. Linear interpolation in n is used for other boundary shapes.

2.7 Non-isotropic Boundary Conditions for Multiregion Calculations

The two-region treatment described in the previous subsection may be applied as an approximation in multiregion calculations. This is a reasonable approach because the intended application is to reactor lattices consisting of fuel, can and moderator. Indeed, the usual application is to a three-region calculation with one mesh interval per material. In such lattices, it is sufficient to distinguish only between fuel and non-fuel when applying anisotropy to the boundary conditions. Therefore a multiregion system has been transformed into a two-region system by volume smearing within the two regions. The treatment of the previous subsection may then be applied to this two-region system to obtain a value of β^*, as given by Equation (40).

Let R_{ij} be the return vector from the boundary for neutrons starting in region i, so that

$$P'_{ij} = P_{ij} + P_{iB}R_{ij} \quad . \tag{41}$$

For a white boundary condition, R_{ij} is independent of i and is given by

$$R_j = \frac{V_j \Sigma_j P_{jB}}{\sum_{k=1}^{N} V_k \Sigma_k P_{kB}} \quad . \tag{42}$$

Let M be the outermost region included in the central region of the two-region calculation. The conditions to be satisfied are:

neutron conservation

$$\sum_{j=1}^{N} R_{ij} = 1 \quad , \tag{43}$$

reciprocity

$$V_i \Sigma_i P_{iB} R_{ij} = V_j \Sigma_j P_{jB} R_{ji} \quad , \tag{44}$$

and

$$\frac{\sum_{j>M} R_{ij}}{\sum_{j\leq M} R_{ij}} = \frac{\beta^* B}{A} \quad , \tag{45}$$

where $A = \underset{j \leqslant M}{\text{Sum}} V_j \Sigma_j P_{jB}$, (46)

and $B = \underset{j > M}{\text{Sum}} V_j \Sigma_j P_{jB}$. (47)

These conditions are satisfied by the equation

$$R_{ij} = \begin{cases} \dfrac{V_j \Sigma_j P_{jB}}{A+\beta^* B} & i \leqslant M,\ j \leqslant M, \\ \dfrac{\beta^* V_j \Sigma_j P_{jB}}{A+\beta^* B} & i \leqslant M,\ j > M \text{ and } i > M,\ j \leqslant M, \\ \left(1 - \dfrac{\beta^* A}{A+\beta^* B}\right) \dfrac{V_j \Sigma_j P_{jB}}{B} & i > M,\ j > M \end{cases} . \quad (48)$$

2.8 Comparison with Numerical Integration

Comparison of the method presented here with results obtained using the numerical integration routines of Doherty [1969] are given in Table 4 for two- and three-region systems in square, hexagonal and circular lattices. The cross sections used are those appropriate to resonance subgroup calculations of ^{238}U oxide rods. The can cross section is 0.0769 cm^{-1}. The comparison is made in terms of the total moderator-to-fuel collision probability. The results are quite good for H_2O moderated systems. There is a deterioration for the very tight D_2O lattice, but this is of little importance to practical systems.

3. CLUSTER GEOMETRY

3.1 General

The system considered is a cluster lattice in which fuel rods are positioned on a number of concentric rings. It is assumed that annuli may be chosen to subdivide the coolant such that a given ring of rods is included in a particular coolant annulus. It is also assumed that it is unnecessary to distinguish between the rods in a given ring. The general approach to the calculation is:

(a) To calculate collision probabilities within the average pincell of each ring of rods by the methods of Section 2.

(b) To define an homogenised cross section for those annuli containing rods in terms of the pincell collision probabilities.

(c) To calculate the collision probabilities for the annuli of the cluster using the homogenised cross sections by the methods of Section 2.

(d) To partition the collision probabilities within each ring of rods using suitable boundary conditions on the pincell calculation (a).

(e) To apply isotropic boundary conditions to the cluster boundary in the usual way.

The method presented differs from that of other authors in its use of a polygonal pincell boundary, in the inclusion of non-isotropic boundary conditions on the pincell, and in the method of partition of collision probabilities.

Discussion of the choice of the coolant annuli between rings of rods is deferred until Section 4. Although it is clear that pincell boundaries in the interior of clusters do have polygonal shapes, precise boundaries are not well defined in most clusters. The exceptions are 7-rod clusters in which the pincell boundary is hexagonal. For other clusters, a value intermediate between squares and hexagons appears most appropriate, therefore a 5-sided boundary has been adopted.

3.2 Calculation of Homogenised Cross Sections

Let V_m^i, Σ_m^i be the volume and cross section for region m of a pincell within the annulus i of the cluster. Let P_{mn}^i denote the probability that a neutron born in region m has its first collision in region n for a pincell within annulus i, where the values of P_{mn}^i are calculated by the methods described in Section 2 for a free boundary. The probability of crossing the pincell boundary P_{mB}^i is given by

$$P_{mB}^i = 1 - \underset{n}{\text{Sum}}\, P_{mn}^i \quad . \tag{49}$$

For isotropic incidence of neutrons on the boundary, the striking probabilities P_{Bm}^i are given by

$$P_{Bm}^i = 4V_m^i \Sigma_m^i P_{mB}^i / S_i \quad , \tag{50}$$

where S_i is the pincell surface.

The homogenised cross section Σ_i is defined to be that cross section which reproduces the total striking probability within the pincell for isotropic incidence of neutrons on the pincell boundary. This assumption is similar to that made by a number of authors, *e.g.* Bollacasa & Bonalumi [1970] and Yamamoto & Ishida [1971]. From Equation (13), the self-collision probability P_i of a homogeneous polygon of cross section Σ_i is given by

$$P_i = P_c(\Sigma_i r^i_{eff}) \quad , \tag{51}$$

where $$r^i_{eff} = r^i_B + (r^i_W - r^i_B)/(1 + \frac{1}{2}\Sigma_i r^i_W) \quad , \tag{52}$$

and r^i_B, r^i_W are the black and white radii of the polygonal pincell respectively. Equating the striking probabilities gives

$$\frac{4(\text{Sum}_m V^i_m)\Sigma_i}{S_i}(1-P_i) = \text{Sum}_m P^i_{Bm} \quad . \tag{53}$$

The required value for Σ_i is obtained from an iterative solution of Equations (51) to (53).

3.3 Partition of the Collision Probabilities

3.3.1 Isotropic boundary conditions on the pincells

The application of isotropic boundary conditions to the pincells is considered first. The several cases which arise are considered in turn. The symbol P'_{ij} denotes the collision probabilities obtained for the annuli of the cluster with homogenised Σ_i using the methods described in Section 2, and P_{ij} denotes the required cluster collision probabilities.

For the case in which the annuli i and j are homogeneous, that is they contain no rods, $P_{ij} = P'_{ij}$ is immediate.

For the case in which annulus i is homogeneous and j contains rods, the probability that a neutron born in annulus i has its first collision in region m of a pincell within annulus j is represented by $P_{i,m(j)}$. Application of the isotropic boundary conditions gives

$$P_{i,m(j)} = \frac{P'_{ij}P^j_{Bm}}{1-P^j_{BB}} \quad , \tag{54}$$

where $$P^j_{BB} = 1 - \text{Sum}_m P^j_{Bm} \quad . \tag{55}$$

For the case in which annulus i contains rods but j does not, reciprocity gives

$$N_i V^i_m \Sigma^i_m P_{m(i),j} = V_j \Sigma_j P_{j,m(i)} \quad , \tag{56}$$

where N_i is the number of rods in annulus i, and V_j is the volume of annulus j. Then

$$P_{m(i),j} = \frac{V_j\Sigma_j P'_{ji}}{N_i V^i_m \Sigma^i_m}\frac{P^i_{Bm}}{1-P^i_{BB}} = \frac{V_i\Sigma_i P'_{ij}}{N_i V^i_m \Sigma^i_m}\frac{P^i_{Bm}}{1-P^i_{BB}} \quad . \tag{57}$$

The application of Equations (50) and (53) gives the simpler expression

$$P_{m(i),j} = \frac{P'_{ij} P^i_{mB}}{1-P_i} \quad . \tag{58}$$

By the application of isotropic boundary conditions to a pincell in annulus j, it follows that when both annulus i and annulus j ($j \neq i$) contain rods

$$P_{m(i),n(j)} = \frac{V_i \Sigma_i P'_{ij}}{N_i V^i_m \Sigma^i_m} \frac{P^i_{Bm}}{1-P^i_{BB}} \frac{P^j_{Bn}}{1-P^j_{BB}} \quad , \tag{59}$$

or

$$P_{m(i),n(j)} = \frac{P'_{ij} P^i_{mB}}{1-P_i} \frac{P^j_{Bn}}{1-P^j_{BB}} \quad . \tag{60}$$

The remaining case is the partition of the probabilities within an annulus i which contains rods. Following Bollacasa & Bonalumi [1970], it is assumed that the probabilities may be written in the form

$$P_{m(i),n(i)} = P^i_{mn} + \rho_i \frac{P^i_{mB} P^i_{Bn}}{1-P^i_{BB}} \quad , \tag{61}$$

where ρ_i is to be determined. That is, of those neutrons which cross the pincell boundary, the fraction which has its next collision in a pincell within the annulus is assumed to be independent of the pincell region m in which it was born. Summing Equation (61) over n gives

$$P_{m(i),i} = 1-P^i_{mB} + \rho_i P^i_{mB} \quad . \tag{62}$$

But since for all $j \neq i$, including those containing rods,

$$P_{m(i),j} = \frac{P^i_{mB}}{1-P_i} P'_{ij} \quad , \tag{63}$$

neutron conservation requires

$$1-P_{m(i),i} = \frac{P^i_{mB}}{1-P_i} (1-P'_{ii}) \quad . \tag{64}$$

Comparison of Equations (62) and (64) gives

$$\rho_i = \frac{P'_{ii}-P_i}{1-P_i} \quad . \tag{65}$$

3.3.2 Non-isotropic boundary conditions on the pincells

Non-isotropic boundary conditions are applied only in those cases in which both annuli i and j contain rods. The self-collision case is considered first. The equation for $P_{m(i),n(i)}$ has the form

$$P_{m(i),n(i)} = P^i_{mn} + \rho_i \frac{P^i_{mB} P^{mi}_{Bn}}{1-P^{mi}_{BB}} \quad , \tag{66}$$

where there is now a distinction between striking probabilities P^i_{Bn}, P^i_{BB} depending on the region m of birth. This equation may be written

$$P_{m(i),n(i)} = P^i_{mn} + \rho_i \alpha^i_{mn} \frac{P^i_{mB} P^i_{Bn}}{1-P^i_{BB}} \quad , \tag{67}$$

where α^i_{mn}, in terms of the return vectors of Section 2.7, is given by

$$\alpha^i_{mn} = R^i_{mn}/R^i_n \quad . \tag{68}$$

That is, for a two-region boundary condition

$$\alpha^i_{mn} = \begin{cases} \dfrac{A+B}{A+\beta^* B} & m \leq M,\ n \leq M, \\ \dfrac{\beta^*(A+B)}{A+\beta^* B} & m \leq M,\ n > M, \text{ and } m > M,\ n \leq M, \\ \left(1 - \dfrac{\beta^* A}{A+\beta^* B}\right) \dfrac{A+B}{B} & m > M,\ n > M, \end{cases} \tag{69}$$

where A, B, β^* depend on i, and A and B are the inner and outer partial summations of $V^i_m \Sigma^i_m P^i_{mB}$, respectively.

These α^i_{mn} cannot be immediately applied to the calculation of $P_{m(i),n(j)}$ for $i \neq j$ because reciprocity demands a value of α_{mn} which is independent of the annulus i or j in which the neutron is born. A suitable choice is

$$P_{m(i),n(j)} = \frac{V_i \Sigma_i P'_{ij}}{N_i V^i_m \Sigma^i_m} \frac{P^i_{Bm}}{1-P^i_{BB}} \frac{P^i_{Bn}}{1-P^j_{BB}} \alpha^{(ij)}_{mn} \quad , \tag{70}$$

where $\alpha^{(ij)}_{mn} = \frac{1}{2}(\alpha^i_{mn} + \alpha^j_{mn})$.

With anisotropic boundary conditions, it is not possible to satisfy the condition

$$\sum_{n} P_{m(i),n(j)} = \frac{P'_{ij} P^{i}_{mB}}{1-P_i} \qquad (71)$$

unless $\alpha^{i}_{mn} = \alpha^{j}_{mn}$. This condition (Equation 71) is necessary for detailed neutron conservation and has been used in the derivation of ρ_i. However, with the above choice of $\alpha^{(ij)}_{mn}$,

$$\sum_{m} \sum_{n} \frac{P^{i}_{Bm}}{1-P^{i}_{BB}} \frac{P^{j}_{Bn}}{1-P^{j}_{BB}} \alpha^{(ij)}_{mn} = 1 \quad . \qquad (72)$$

Therefore $$\sum_{m} \sum_{n} N_i V^{i}_{m} \Sigma^{i}_{m} P_{m(i),n(j)} = V_i \Sigma_i P'_{ij} \quad , \qquad (73)$$

or $$\sum_{m} V^{i}_{m} \Sigma^{i}_{m} P_{m(i),j} = \frac{\sum_{m} V^{i}_{m} \Sigma^{i}_{m} P^{i}_{mB}}{1-P_i} P'_{ij} \quad . \qquad (74)$$

Then neutron conservation for annuli of the cluster gives

$$\sum_{m} V^{i}_{m} \Sigma^{i}_{m} (1-P_{m(i),i}) = \frac{\sum_{m} V^{i}_{m} \Sigma^{i}_{m} P^{i}_{mB}}{1-P_i} (1-P'_{ii}) \quad . \qquad (75)$$

An alternative expression is obtained by multiplying Equation (67) by $V^{i}_{m} \Sigma^{i}_{m}$ and summing over m and n, which gives

$$\sum_{m} V^{i}_{m} \Sigma^{i}_{m} (1-P_{m(i),i}) = (1-\rho_i) \sum_{m} V^{i}_{m} \Sigma^{i}_{m} P^{i}_{mB} \quad . \qquad (76)$$

Therefore

$$\rho_i = \frac{P'_{ii}-P_i}{1-P_i} \quad , \qquad (77)$$

as before.

4. COMPARISON WITH NUMERICAL SOLUTIONS FOR CLUSTERS

4.1 General

Comparison of the present synthetic treatment of clusters has been made with the numerical method of Doherty [1970]. The clusters considered are 7- and 19-rod clusters with D_2O coolant, and a 36-rod cluster for a steam generating heavy water (SGHW) reactor system with H_2O or air coolant. A complete description of the geometry of each cluster is given in Tables 5 to 7. Each of the clusters consists of a number of

rings of rods with the rods equally spaced on each ring. The rod positions are therefore completely specified by the radius of the pitch circle, the number of rods in the ring and the angular displacement of one of the rods from a reference diameter of the cluster.

The comparison has been made for two types of calculation. In the first, a few-group cell calculation has been performed using cross sections generated by the AUS scheme [Robinson 1975]. In the second, a calculation of the resonance subgroup type has been performed under the assumptions of narrow resonance theory. Such a subgroup calculation is made when applying the method in the AUS module MIRANDA [Robinson 1977].

The numeric method may be described briefly as the setting out of parallel neutron tracks across the cluster at a number of orientations to a reference diameter and integration along each track to produce collision probabilities for the different regions. In the routine of Doherty [1970], the number of lines per annulus is a constant and the angular integration ranges from 0 to 2π. Thus the number of angles should be prime with respect to the number of rods on any ring. The number of lines and angles used in each case is specified later.

4.2 Coolant Annuli for the Synthetic Method

When applying the synthetic method, it is necessary to choose annuli which divide the coolant so that a ring of rods is associated with a particular annulus. Variation in the chosen annuli may have a considerable effect on the final results. The annuli for this work have been chosen by a combination of two principles. The first principle has been applied to the inner rod rings where it is possible to identify natural polygonal boundaries of the pincells. The coolant annuli are then chosen to preserve the pincell volume. The second principle, which has been applied to the outer rings, is to maintain the same average radius of fuel material in the smeared annulus as in the ring of rods. That is

$$\frac{2}{3}\,\frac{r_i^3-r_{i-1}^3}{r_i^2-r_{i-1}^2} = \frac{\int_{rod} r\,dv}{\int_{rod} dv}\,, \qquad (78)$$

where r_i are the required coolant annuli and r is the distance from the cluster centre of the elemental volume, dv. Equation (78) has been applied by working outward from the chosen inner annuli.

The 7-rod cluster may be considered as part of an infinite array of hexagonal pincells. Thus the first principle gives coolant annuli of radius 1.400275 and 3.70478 cm. The coolant-to-fuel ratio is 0.2416 in both annuli.

For the 19-rod cluster, the two innermost annuli have been chosen using the first principle. The pincell boundaries are depicted in Figure 2 for a 60° sector of the cluster in which only the rod centres are marked. The boundaries have been deduced from the facts that:

(a) A, B, C form an equilateral triangle of side 1.65 cm.

(b) B, C, D, E form an approximate square of side 1.65 cm.

(c) B, E, F form half an approximate equilateral triangle of side 1.65 cm.

Thus the first two radii become 0.86736 and 2.3697 cm. Using the second principle, the outer radius becomes 3.9226 cm. The coolant-to-fuel ratios for the three annuli are 0.3466, 0.4621 and 0.4695.

The central 'rod' and the two inner rings of the 36-rod cluster are very similar to those of the 19-rod cluster and the radii have been deduced in the same way. The second principle has been used for the outermost radius. This gives coolant radii of 0.99678, 2.7093, 4.4642 and 6.3799 cm. The corresponding coolant-to-fuel ratios are 0.8153, 0.7986 and 0.9991.

4.3 Few-group Lattice Calculations

The calculations have been performed in four groups with energy boundaries at 0.82 MeV, 5.53 keV and 0.62 eV. The 4-group data were prepared by using the AUS modular scheme and, in fact, a synthetic collision probability method was employed in deriving the cross sections. Four-group calculations were chosen to minimise computer time for the numeric calculations and still represent the main effects. The results have been presented as k_{inf}, k_{eff} and region average fluxes for the fast and thermal groups. The flux is normalised to a fission source of ten neutrons. The k_{eff} has been deduced by applying a simple DB^2 leakage term without a streaming correction. Both coolant and moderator have been sufficiently subdivided in the numeric solution to obtain a 'best' solution for comparison with the synthetic method.

4.3.1 Seven-rod cluster

The numeric routine was used with 11 angles, 8 lines per annulus and annular mesh intervals of 1.2, 0.07, 0.130275, 3 of 0.768, 0.42322, 0.089 and 20 of 0.36669 cm. The fuel was not subdivided by radii of the

rods, but by radii defining the coolant annuli of the cluster. The synthetic routine was used with an hexagonal interpin boundary and annular mesh intervals of 1.400275, 2.304505, 0.42322, 0.089 and 10 of 0.73338 cm. The results are given in Table 8. The reactivity agreement is excellent. The worst flux discrepancy is 4 per cent in the fast flux in the fuel rods. One of the most important quantities is the moderator thermal flux which is 1 per cent in error.

4.3.2 Nineteen-rod cluster

The numeric routine was used with 5 angles, 8 lines per annulus and annular mesh intervals of 0.71, 0.05, 0.10736, 2 of 0.71373, 2 of 0.742955, 0.34927, 0.265, 0.685, 0.14 and 10 of 0.63308 cm. The cluster annuli again subdivided the rods. The synthetic routine was used with a pentagonal interpin boundary; four of the mesh intervals were 0.86736, 1.50234, 1.5529 and 0.2074 cm and the remainder were as for the numeric solution. The results are given in Table 9. The agreement is very similar to that for the 7-rod cluster.

4.3.3 Thirty-six-rod cluster

The H_2O-cooled cluster situation is very different from that for the D_2O-cooled clusters. In this case, there are large flux gradients in the coolant at thermal energies; therefore it is not possible to obtain the reactivity of the lattice to better than about 1 per cent unless the coolant associated with each ring of rods is subdivided. The synthetic method is not directly applicable with subdivided coolant rings. However, reasonable accuracy is attained by using the synthetic routine to calculate fluxes for use in smearing the fuel, can and coolant within each of the annuli encompassing a rings of rods. These smeared cross sections are then used in a cylindrical calculation of the cluster using collision probability or discrete ordinate methods. In the results given here, the discrete ordinate module ANAUSN [B.E. Clancy, G. Doherty & G.S. Robinson, AAEC report in preparation] has been applied in the S_{16} approximation.

For the water-cooled case, a direct comparison of the synthetic method has been made with a numeric solution using the same undivided coolant annuli. The numeric solution with divided coolant annuli has been compared with the ring smearing model. The results are given in Table 10. The numeric routine was used with 5 angles and 8 lines in both calculations. The mesh intervals for undivided coolant were 0.794, 0.20278, 1.71252, 1.7549, 1.9157, 0.1481, 0.429, 1.9255, 0.325

and 8 of 0.6855 cm. For divided coolant, the cluster mesh intervals were 0.794, 0.20278, 4 of 0.4072, 2 of 0.4744, 4 of 0.2372, 8 of 0.2262 and 0.1948 cm. The difference obtained by reducing the maximum mesh interval in the outer one and a half rings from 0.47 cm to 0.24 cm was 0.1 per cent in k_{eff}. These mesh intervals were also allowed to subdivide the fuel, but the total effect for this subdivision was only 0.1 per cent in k_{eff}. An S_N calculation requires fewer mesh points in the cluster, but more in the insulating gap. The mesh intervals were 0.794, 0.20278, 4 of 0.42813, 4 of 0.438725, 4 of 0.478925, 0.1481, 0.429, 5 of 0.3851, 0.325 and 8 of 0.6855 cm. It may be seen from Table 10 that, although the flux distribution within the fuel rods is rather inaccurate, the overall results obtained by ring smearing are much improved on the direct synthetic solution.

The 36-rod cluster has also been calculated for voided coolant. The difficulties associated with water coolant do not arise, but both the synthetic and ring smearing results are presented in Table 11, because a consistent calculation method is required. The same mesh intervals as for H_2O coolant were used, except within the rod cluster for the numeric solution. These mesh intervals were set at 0.794, 1.1045, 1.7415, 1.584, 0.482 and 0.822 in order to give some fuel subdivision. The results, both with and without ring smearing, are much better than those for water coolant.

4.4 Resonance Subgroup Calculations

Comparisons of the synthetic method with numerical results have also been made for calculations of the resonance subgroup type. Under the assumptions of narrow resonance theory, these calculations are particularly simple. The equations to be solved for the resonance flux depression ϕ_i in fuel regions are

$$V_i \Sigma_i' \phi_i = \sum_j P_{ji}\{\Sigma_i'\} V_j \Sigma_j \quad , \tag{79}$$

where Σ_i is the macroscopic potential scattering cross section,

Σ_i' is the macroscopic cross section including the resonance subgroup cross section, and

$P_{ji}\{\Sigma_i'\}$ is the collision probability.

The accuracy of these comparisons gives a useful indication of the accuracy of the collision probability evaluation for general resonance subgroup calculations.

The comparisons have been made for the three cluster types using potential scattering cross sections of 0.42457, 0.0769, 0.08442, 0.35238, 1.4087 and 1.0618 cm^{-1} for the fuel, can, tubes, D_2O, H_2O and SGHW central rod, respectively. The total cross sections of the fuel were 0.42457, 0.48289, 1.3577, 15.354 and 239.3 cm^{-1} for the five subgroups considered. The mesh intervals used in the synthetic calculations were the same as those of the previous subsection, except for the use of five moderator mesh intervals. In fact, one interval would suffice as the source is constant. The mesh intervals used in the numeric calculations were the same as those for the synthetic calculations except that the central rod region of the 7- and 19-rod clusters was represented by three discrete annuli. The number of lines per annulus was increased to 16 because the annuli were wider than those used previously. The number of angles was maintained.

The results are given in Tables 12 to 14 for 7-, 19- and 36-rod calculations, respectively. The agreement at low resonance cross sections is very good for all clusters. This is not surprising because for zero resonance cross section (subgroup 1) any collision probabilities having neutron conservation and reciprocity properties give the correct constant flux distribution. In fact, the synthetic method is slightly better than the numeric results in this respect.

The agreement is not as good for large resonance cross sections. However, the most important quantity, the fuel average flux, is calculated to better than 0.5 per cent except for the 7-rod cluster. It should be noted that the 7-rod cluster has a small number of very large rods with a low coolant-to-fuel ratio. The inclusion of non-isotropic pincell boundary conditions has most effect for the H_2O-cooled cluster. Use of the isotropic boundary conditions on circular pincell boundaries resulted in a 1.8 per cent overestimate of the average fuel flux in this case. For large resonance cross sections, the fuel flux distribution is accurate to 1 to 2 per cent, except for the voided case. For all clusters, there appears to be an underestimation of the probability that a moderator neutron which enters the cluster has a collision in the outermost ring of rods, rather than in the internal rods. This underestimation is accentuated in the case of black rods in a voided cluster. The agreement obtained for all clusters is quite satisfactory for resonance calculations.

5. CONCLUSIONS

The approximate methods which have been developed provide fast, accurate evaluation of collision probabilities for neutrons in cylindrical and cluster geometries. The inclusion of non-isotropic boundary conditions makes the routines particularly suitable for resonance calculations in which pincell boundary shapes must be considered.

It has been noted by many authors that Bonalumi-type approximations in cylindrical geometry tend to break down for very fine mesh subdivision. Continued mesh refinement to improve the spatial flux representation leads to worse rather than better results. This restriction also applies to the present synthetic method for clusters, but numerical calculations are very slow and the synthetic method must be applied in all but a few check calculations.

The methods have been incorporated in two modules of the AUS scheme: the MIRANDA module for resonance calculations and the general purpose collision probability module ICPP [Clancy *et al.*, AAEC report in preparation].

6. REFERENCES

Bollacasa, D. & Bonalumi, R.A. [1970] - A method to calculate collision probabilities in clusters. *Energ. Nucl. (Milan)*, 17 : 244.

Bonalumi, R.A. [1961] - Neutron first collision probabilities in reactor physics. *Energ. Nucl. (Milan)*, 8 : 326.

Bonalumi, R.A. [1965] - Systematic approximations in neutron first collision probabilities. *Energ. Nucl. (Milan)*, 12 : 1.

Case, K.M., de Hoffman, F. & Placzek, G. [1953] - Introduction to the Theory of Neutron Diffusion. Vol.1, Los Alamos Monogr. US Government Printing Office, Washington, DC.

Doherty, G. [1969] - Some methods of calculating first flight collision probabilities in slab and cylindrical lattices. AAEC/TM489.

Doherty, G. [1970] - Collision probability calculations in cluster geometry. AAEC/E205.

Jonsson, A. [1963] - THESEUS — a one group collision probability routine for annular systems. AEEW-R253.

Robinson, G.S. [1975] - AUS — the Australian modular scheme for reactor neutronics computations. AAEC/E369.

Robinson, G.S. [1977] - AUS module MIRANDA — a data preparation code based on multiregion resonance theory. AAEC/E410.

Yamamoto, K. & Ishida, M. [1971] - A new approximation in the calculation of collision probabilities in cluster type fuel lattices. *J. Nucl. Sci. Technol.*, 8 : 458.

TABLE 1

COMPARISON OF $P_{ii}^{(o)}$

$\Sigma_i r_i$	r_{i-1}/r_i	$P_{ii}^{(o)}$		
		Numerical Integration	Schaefer Prescription	Bonalumi (Equation 15)
0.0625	0.2	0.07193	0.07202	0.07263
0.0625	0.6	0.04942	0.04949	0.05318
0.0625	0.95	0.01035	0.01001	0.01277
0.25	0.2	0.23784	0.23831	0.23875
0.25	0.6	0.17125	0.17190	0.17473
0.25	0.95	0.03836	0.03802	0.03098
1.0	0.2	0.58026	0.58110	0.58031
1.0	0.6	0.46658	0.46936	0.46251
1.0	0.95	0.13237	0.13097	0.09482
4.0	0.2	0.87138	0.87146	0.87141
4.0	0.6	0.80909	0.81088	0.80857
4.0	0.95	0.36969	0.36651	0.33630
16.0	0.2	0.96746	0.96748	0.96747
16.0	0.6	0.95120	0.95125	0.95121
16.0	0.95	0.71087	0.71663	0.70123

TABLE 2

COMPARISONS OF G_{12}

$\Sigma_2 r_2$	r_1/r_2	G_{12}		Numerical Integration Values of $P_{12}/(1-P_{11})$	
		Numerical Integration	P-L Approximation	$\Sigma_1 = 0$	$\Sigma_1 = \Sigma_2$
0.0625	0.2	0.06396	0.06396	0.07494	0.07411
0.0625	0.6	0.03617	0.03619	0.04134	0.04029
0.0625	0.95	0.00551	0.00552	0.00597	0.00570
0.25	0.2	0.22923	0.22929	0.25609	0.25112
0.25	0.6	0.13559	0.13587	0.15049	0.14291
0.25	0.95	0.02179	0.02186	0.02340	0.02147
1.0	0.2	0.63370	0.63408	0.66191	0.65020
1.0	0.6	0.43167	0.43407	0.45430	0.43262
1.0	0.95	0.08331	0.08410	0.08767	0.07994
4.0	0.2	0.97724	0.97755	0.97981	0.97762
4.0	0.6	0.87962	0.88549	0.88613	0.87809
4.0	0.95	0.28416	0.29174	0.29091	0.28102
16.0	0.2	1	1	1	1
16.0	0.6	0.99954	0.99971	0.99955	0.99953
16.0	0.95	0.70441	0.73414	0.70717	0.70430

TABLE 3

COMPARISONS OF DANCOFF EFFECT G_m

Lattice	V_2/V_1	τ†	$y = \frac{4V_2\Sigma_2}{S_1}$	G_m Values		
				Monte Carlo	Bonalumi (1965)	This Work
Square	0.2732	0	0.2587	0.2005±0.0005	0.1979	0.1980
"	0.2732	0	0.6207	0.362 ±0.001	0.3609	0.3609
"	0.6	0.202	0.5685	0.372 ±0.001	0.3630	0.3718
"	0.6	0.202	1.3643	0.609 ±0.003	0.6223	0.6039
"	1.0	0.253	0.9474	0.521 ±0.002	0.5064	0.5187
"	1.0	0.253	2.2738	0.778 ±0.005	0.7831	0.7621
"	3.0	0.258	2.8423	0.826 ±0.006	0.8195	0.8266
"	3.0	0.258	6.8214	0.976 ±0.009	0.9677	0.9650
Hexagonal	1.0	0.347	0.9474	0.526 ±0.002	0.5317	0.5260
"	1.0	0.347	2.2738	0.783 ±0.005	0.7642	0.7792
"	3.0	0.302	2.8423	0.821 ±0.006	0.8312	0.8307
"	3.0	0.302	6.8214	0.960 ±0.011	0.9642	0.9687

† $\tau = TS_1/4V_2$ where T is the minimum surface-to-surface distance between rods.

TABLE 4

COMPARISONS OF MODERATOR-TO-FUEL PROBABILITY

Case Description	Σ_{fuel}	Values of $P_{mod \to fuel}$					
		Square		Hexagonal		Circular White	
		Numerical	% Error	Numerical	% Error	Numerical	% Error
r_i = 0.25,0.35355	0.42457	0.20579	-0.3	0.20683	-0.3	0.20857	-0.4
H_2O	1.3577	0.40511	-0.7	0.40773	-0.5	0.41322	-0.4
Σ_m = 1.48	239.3	0.60420	+0.6	0.61377	+0.3	0.63203	-0.4
r_i = 0.5,0.7071	0.42457	0.19169	-0.9	0.19310	-0.8	0.19445	-0.3
H_2O	1.3577	0.34448	-0.9	0.34850	-0.7	0.35579	0.0
Σ_m = 1.48	239.3	0.44060	-0.9	0.44869	-1.0	0.46074	-0.2
r_i = 0.724,0.794,1.049	0.42457	0.19027	-0.2	0.19281	-0.5	0.19590	-0.3
H_2O	1.3577	0.31052	+0.3	0.31700	-0.1	0.32612	+0.1
Σ_m = 1.4807	239.3	0.36103	+0.7	0.37135	-0.2	0.38387	+0.1
r_i = 0.724,0.794,1.049	0.42457	0.4850	+0.2	0.4884	+0.2	0.4964	-0.6
D_2O	1.3577	0.6343	+1.6	0.6414	+1.5	0.6599	-0.2
Σ_m = 0.35238	239.3	0.6778	+2.6	0.6914	+1.7	0.7135	-0.2

TABLE 5

7-ROD CLUSTER SPECIFICATIONS

Rod layout:	central rod + 6 rods on pitch circle of radius 2.667 cm
Fuel material:	Natural UO_2, density 10.2 g cm^{-3}
Fuel diameter:	2.4 cm
Cladding material:	73.5% Al, 26.5% void
Cladding diameter:	inner 2.4 cm, outer 2.54 cm
Shroud material:	Al
Shroud diameter:	inner 8.256 cm, outer 8.434 cm
Coolant:	D_2O 99.73%, H_2O 0.27%
Moderator:	D_2O 99.73%, H_2O 0.27%
Lattice pitch (hexagonal):	22 cm
Temperature:	$20^{o}C$
Buckling:	5.97 m^{-2}

TABLE 6

19-ROD CLUSTER SPECIFICATIONS

Rod layout:	central rod + 6 rods on pitch circle of radius 1.65 cm + 12 rods on pitch circle of radius 3.19 cm, angular displacement of 15°
Fuel material:	natural UO_2, density 10.45 g cm^{-3}
Fuel diameter:	1.42 cm
Cladding material:	90.3% Al, 9.7% void
Cladding diameter:	inner 1.42 cm, outer 1.52 cm
Pressure tube material:	Al
Pressure tube diameter:	inner 8.26 cm, outer 8.79 cm
Calandria tube material:	Al
Calandria tube diameter:	inner 10.16 cm, outer 10.44 cm
Coolant:	99.63% D_2O, 0.37% H_2O
Insulating gap:	void
Moderator:	99.63% D_2O, 0.37% H_2O
Lattice pitch (hexagonal):	22 cm
Temperature:	20 °C
Buckling:	3.804 m^{-2}

TABLE 7

36-ROD CLUSTER SPECIFICATIONS

Rod layout:	6 rods on pitch circle of radius 1.8985 cm + 12 rods on pitch circle of radius 3.64 cm, angular displacement 15^{o} + 18 rods on pitch circle of radius 5.466 cm, angular displacement zero
Fuel material:	UO_2, 1.35% enrichment, density 10.45 g cm^{-3}
Fuel diameter:	1.448 cm
Cladding material:	91.1% Al, 8.9% void
Cladding diameter:	inner 1.448 cm, outer 1.588 cm
Central 'rod' material:	70% H_2O, 30% Al
Central 'rod' diameter:	1.588 cm
Pressure tube material:	Al
Pressure tube diameter:	inner 13.056 cm, outer 13.914 cm
Calandria tube material:	Al
Calandria tube diameter:	inner 17.765 cm, outer 18.415 cm
Coolant:	H_2O or void
Insulating gap:	void
Moderator:	99.63% D_2O, 0.37% H_2O
Lattice pitch (square):	26.04 cm
Temperature:	$20^{o}C$
Buckling:	8 m^{-2}

TABLE 8

7-ROD FEW-GROUP CALCULATIONS

Quantity	Numeric	Synthetic	% Error
k_{inf}	1.14802	1.14873	0.06
k_{eff}	0.99788	0.99787	0.0
Region average flux:			
centre fuel, fast	0.883	0.901	2.0
thermal	1.521	1.560	2.6
ring 1 fuel, fast	0.764	0.792	3.7
thermal	1.818	1.807	-0.6
coolant, fast	0.5346	0.5443	1.8
thermal	2.148	2.159	0.5
tube, fast	0.3947	0.3964	0.4
thermal	2.424	2.389	-1.4
moderator, fast	0.1529	0.1509	-1.3
thermal	3.159	3.190	1.0

TABLE 9

19-ROD FEW-GROUP CALCULATIONS

Quantity		Numeric	Synthetic	% Error
k_{inf}		1.09184	1.09238	0.05
k_{eff}		0.99333	0.99348	0.015
Region average flux:				
centre fuel,	fast	0.848	0.838	-1.2
	thermal	1.542	1.574	2.0
ring 1 fuel,	fast	0.810	0.828	2.3
	thermal	1.639	1.650	0.7
ring 2 fuel,	fast	0.696	0.717	3.0
	thermal	1.943	1.931	-0.6
coolant,	fast	0.5903	0.6023	2.0
	thermal	2.037	2.047	0.5
pressure tube,	fast	0.4044	0.4131	2.2
	thermal	2.419	2.409	-0.4
calandria tube,	fast	0.3244	0.3224	-0.6
	thermal	2.499	2.496	-0.1
moderator,	fast	0.1628	0.1609	-1.1
	thermal	3.016	3.045	1.0

TABLE 10

36-ROD H_2O COOLANT FEW-GROUP CALCULATIONS

Quantity		Undivided Coolant		Divided Coolant	
		Numeric	Synthetic	Numeric	Synthetic
k_{inf}		1.18645	1.18279	1.17628	1.17514
k_{eff}		1.04230	1.03750	1.02783	1.02592
Region average flux:					
ring 1 fuel,	fast	0.4007	0.4057	0.3851	0.3801
	thermal	0.4112	0.3978	0.3660	0.3490
ring 2 fuel,	fast	0.4019	0.4112	0.3912	0.3872
	thermal	0.4619	0.4503	0.4220	0.4055
ring 3 fuel,	fast	0.3628	0.3707	0.3672	0.3628
	thermal	0.5922	0.5975	0.6175	0.6324
coolant,	fast	0.3081	0.3158	0.3067	0.3045
	thermal	0.6150	0.6226	0.6246	0.6291
pressure tube,	fast	0.2072	0.2136	0.2098	0.2195
	thermal	0.8976	0.9267	1.0000	1.0075
calandria tube,	fast	0.1513	0.1492	0.1527	0.1567
	thermal	0.9354	0.9693	1.0345	1.0449
moderator,	fast	0.0952	0.0930	0.0958	0.0965
	thermal	1.0687	1.1079	1.1674	1.1771

TAELE 11

36-ROD AIR COOLANT FEW-GROUP CALCULATIONS

Quantity		Numeric	Synthetic	Synthetic + smear
k_{inf}		1.22752	1.22821	1.22748
k_{eff}		0.96440	0.96462	0.96372
Region average flux:				
ring 1 fuel,	fast	0.5189	0.5265	0.5293
	thermal	0.4273	0.4333	0.4230
ring 2 fuel,	fast	0.5128	0.5219	0.5170
	thermal	0.4613	0.4643	0.4607
ring 3 fuel,	fast	0.4546	0.4639	0.4556
	thermal	0.5718	0.5668	0.5721
pressure tube,	fast	0.3024	0.3124	0.3094
	thermal	0.7404	0.7321	0.7401
calandria tube,	fast	0.2184	0.2166	0.2208
	thermal	0.7988	0.7968	0.8030
moderator,	fast	0.1336	0.1327	0.1331
	thermal	0.9939	1.0007	1.0014

TABLE 14

36 ROD SUBGROUP CALCULATIONS

Sub-group	Flux Depression, ϕ_i							
	Ring 1		Ring 2		Ring 3		Fuel Average	
	Num.	Syn. Err %	Num.	Syn. Err %	Num.	Syn. Err %	Num.	Syn. Err %
	H_2O Coolant							
1	0.9994	0.1	0.9999	0.0	0.9994	0.1	0.9996	0.0
2	0.9494	0.0	0.9493	-0.1	0.9531	0.1	0.9512	0.0
3	0.5321	-0.2	0.5270	-0.5	0.5519	0.4	0.5403	0.0
4	0.05986	-0.2	0.05888	-0.9	0.06350	0.3	0.06135	-0.2
5	0.003897	-0.2	0.003833	-0.9	0.004138	0.3	0.003996	-0.2
	D_2O Coolant							
1	1.0002	0.0	1.0007	-0.1	0.9996	0.0	1.0001	0.0
2	0.9302	-0.1	0.9306	-0.2	0.9403	0.0	0.9354	-0.1
3	0.4425	0.2	0.4356	0.0	0.4949	-0.3	0.4664	-0.1
4	0.04516	0.5	0.04299	1.1	0.05399	-0.7	0.04885	0.0
5	0.002927	0.6	0.002785	1.1	0.003511	-0.7	0.003172	0.0
	Air Coolant							
1	1.0010	-0.1	1.0014	-0.1	1.0000	0.0	1.0006	0.0
2	0.9118	-0.1	0.9126	-0.2	0.9269	-0.1	0.9196	-0.1
3	0.3670	0.9	0.3624	1.2	0.4466	-0.9	0.4053	0.0
4	0.03375	1.7	0.03140	4.5	0.04684	-2.0	0.03951	+0.3
5	0.002174	1.8	0.002020	4.6	0.003040	-2.1	0.002556	+0.2

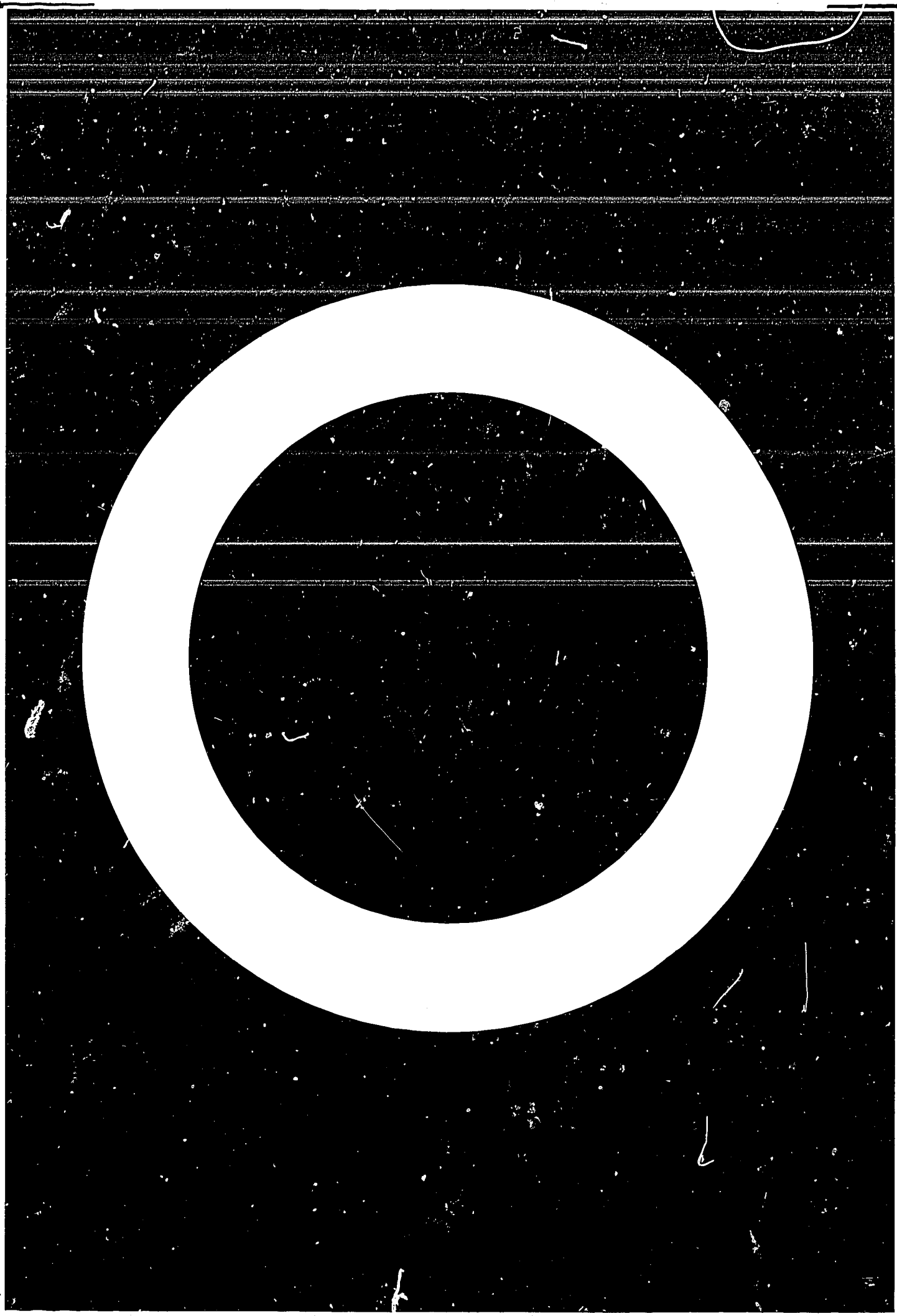

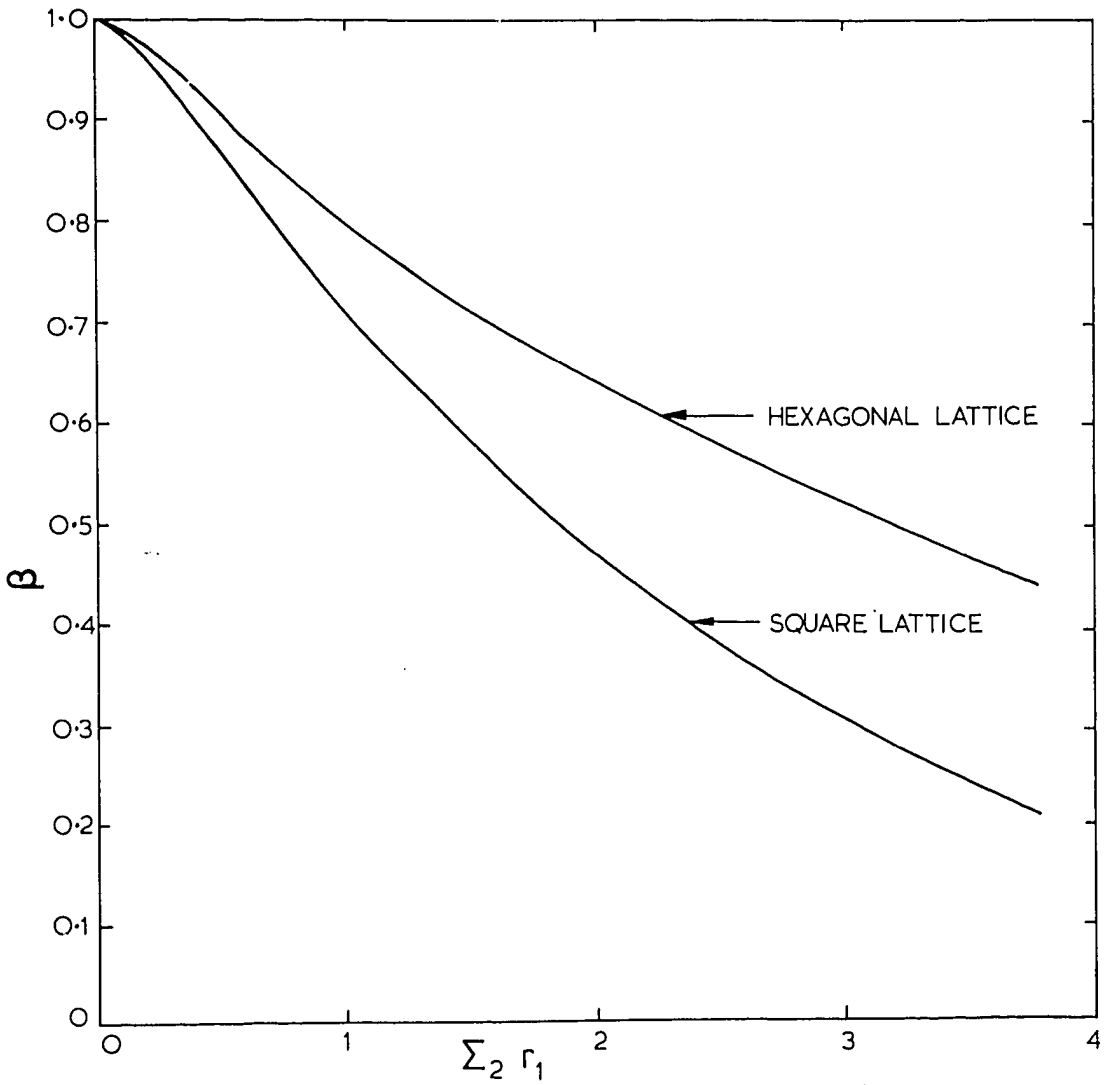

FIGURE 1. VALUES OF β AS A FUNCTION OF $\Sigma_2 r_1$

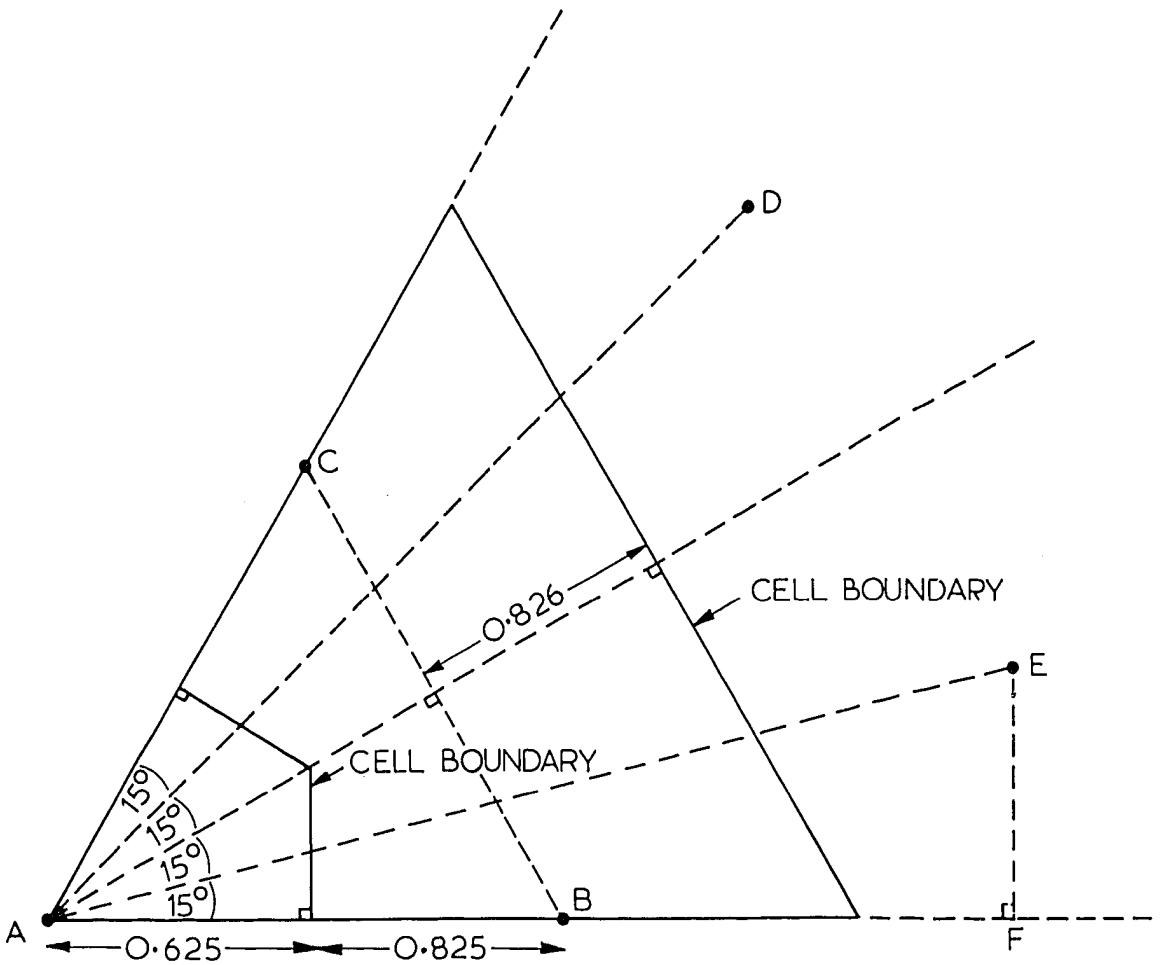

A central rod
B,C rod on pitch circle radius of 1·65 cm.
D,E rods on pitch circle radius of 3·19 cm.

Dimensions in cm

FIGURE 2. SECTOR OF 19–ROD CLUSTER

Printed by the AAEC Research Establishment

C-63

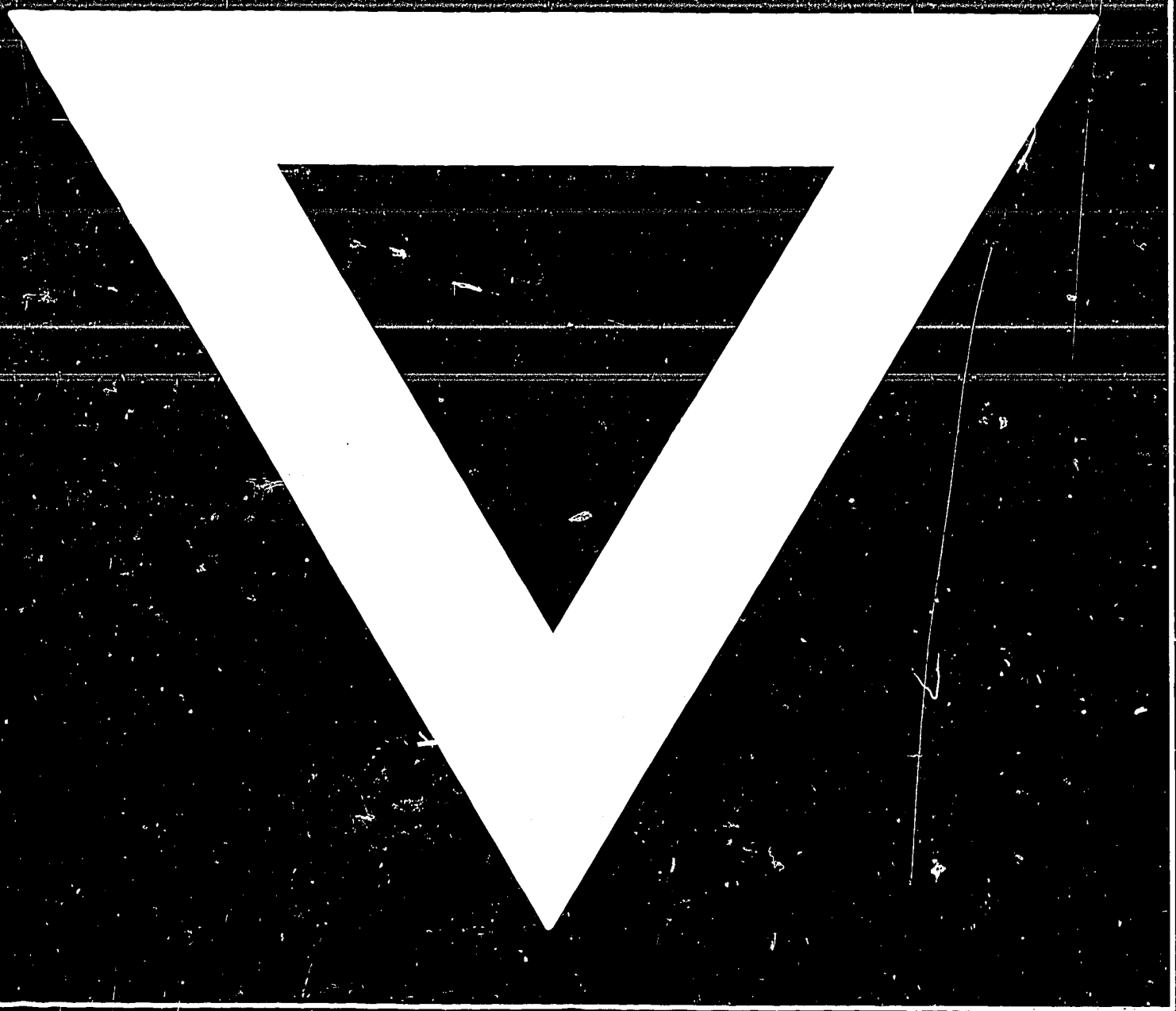

80.01.21